



Diurnal variability of the Atmospheric Boundary Layer height over a tropical station in the Indian Monsoon Region

5 Sanjay Kumar Mehta¹, Madineni Venkat Ratnam², Sukumarapillai V. Sunilkumar³,
Daggumati Narayana Rao¹, and Boddapati V. Krishna Murthy¹

¹SRM Research Institute, SRM University, Kattankulathur-603203, India

²National Atmospheric Research Laboratory, Gadanki-517112, India

³Space Physics Laboratory (SPL), VSSC, Trivandrum- 695022, India

10

Correspondence to: Sanjay Kumar Mehta (sanjaykumar.r@res.srmuniv.ac.in;ksanjaym@gmail.com)

Abstract. The diurnal variation of atmospheric boundary layer (ABL) height is studied using high resolution radiosonde observations available at every 3-h intervals for 3 days continuously from 34 intensive campaigns conducted during the period December 2010-March 2014 over a tropical station
15 Gadanki (13.5° N, 79.2° E), in the Indian monsoon region. The heights of the ABL during the different stages of its diurnal evolution, namely, the convective boundary layer (CBL), the stable boundary layer (SBL), and the residual layer (RL) are obtained to study the diurnal variability. A clear diurnal variation in 9 campaigns is observed while in 7 campaigns the SBL does not form for the entire day and in the remaining 18 campaigns the SBL form intermittently. The SBL forms for 33%-55% of the time during
20 nighttime and 9% and 25% during the evening and morning hours, respectively. The mean SBL height is within 0.3 km above the surface which increases slightly just after midnight (0200 IST) and remains almost steady till morning. The mean CBL height is within 3.0 km above the surface which generally increases from morning to evening. The mean RL height is within 2 km above the surface which generally decreases slowly as the night progresses. Diurnal variation of the ABL height over the Indian
25 region is stronger during the pre-monsoon and weaker during winter season. The CBL is higher during the summer monsoon and lower during the winter season while the RL is higher during winter season and lower during summer season. During all the seasons, the ABL height peaks during the afternoon (~1400 IST) and remains elevated till evening (~1700 IST). The ABL suddenly collapses at 2000 IST and increases slightly over night. Interestingly, it is found that the low level clouds have an effect on the ABL
30 height variability, but not the deep convective clouds.

1 Introduction

Atmospheric boundary layer (ABL) is the lowest layer of the troposphere in which the flow field is directly influenced by the interaction of the Earth's surface at a response time scale of about an hour or less (Stull 1998, Garratt, 1994). The importance of the ABL stems from the fact that it is the gateway for



35 the pollutants and anthropogenic emissions, moisture, heat and momentum fluxes to the free atmosphere.
Rapid transport in the ABL takes place in order to achieve the radiative balance between earth surface and
the free atmosphere. The ABL is the largest sink for atmospheric kinetic energy. The ABL height is one
of the key parameters which provides length scale for the vertical extent and concentration of atmospheric
pollutants, convection activity, and cloud and fog formation (Deardorff, 1972; Holtslag and Nieuwstadt,
40 1986; Seibert et al., 2000; Konor et al., 2009). The diurnal variability is a dominant feature of the ABL,
which plays an important role in the exchanges of heat, momentum, moisture, and chemical constituents
between the surface and free atmosphere.

Depending on the physical process, the diurnal pattern of the ABL is mainly classified into three
major layers: the convective boundary layer (CBL), the stable boundary layer (SBL), and the residual
45 layer (RL) (Stull, 1988; Garratt, 1994). The CBL evolves during the daytime just after the sunrise due to
convective turbulence (thermals of warmer air) associated with entrainment zone, a stable layer, on its top.
Just before the sunset and during night, as the thermals cease to develop, the CBL collapses and the SBL
forms due to fast cooling of the surface. Even though thermals cease to develop during nighttime the
mean state variables remain nearly the same as the former CBL, creating the RL associated with capping
50 inversion layers, a stable layer, on its top. Thus, the RL is disconnected from the ground by underlying
SBL having no source of turbulence generation for its maintenance rather turbulence decays
homogeneously in all directions. Generally, the mean ABL height lies between 0.03 - 3.0 km above the
surface (Stull, 1988). However, the CBL can be as high as ~ 5.0 km during a midsummer day in low-
latitude deserts and as low as ~ 0.5 km m over the ocean. The SBL height generally is less than 0.5 km
55 above the surface (Garratt, 1992).

Diurnal variability of the ABL is not only determined by the variabilities in the surface fluxes, but also
on meteorological conditions such as the presence of the clouds, horizontal advection of air and
subsidence from aloft. These forcings considerably affect turbulence development and the growth of the
ABL. As, for example, the presence of clouds greatly influences the turbulent structure due to local
60 radiative heating or cooling. The diurnal variation is generally strong, mainly over land in the absence of
any upper level cloud and at the time of year when surface temperatures are the highest (Angevine et al.,
2001).

The ABL height is often determined from the vertical profiles of temperature, humidity, and wind
components obtained from radiosonde measurements. Most of the routine radiosondes only operate twice
65 a day at 0000 and 1200 UTC, which are not suited well to study the diurnal variations of the ABL height.
Thus, there have been only a few studies on diurnal variability of the ABL height (Angevine et al., 2001)
mainly due to non-availability of the required measurements with adequate time resolution. High
resolution radiosondes launched at sufficiently close time intervals (less than 1-h) can provide direct
information on diurnal variability of ABL height. Liu and Liang (2010) studied the climatology of the
70 ABL height diurnal cycle, using fine-resolution soundings launched at intervals ranging from 1-12 hours
collected in 14 major field campaign around the world. They found a strong diurnal cycle, both over land



and oceans, whereas the cycle is weak over ice. Seidel et al., (2010) using routine radiosondes over the globe found significant differences in day and night ABL heights.

Recently, various remote sounding systems such as lidar (Tucker et al., 2009), sodar (Shravan Kumar and Anandan, 2009), wind profiler (Kumar and Jain, 2006; Bianco et al., 2011), Radio Acoustic Sounding System (RASS) (Clifford et al., 1994; Chandrasekhar Sarma et al., 2008), ceilometer (van der Kamp and McKendry, 2010) have been developed for continuous direct measurements or estimates to study the diurnal variation of the ABL height (Seibert et al., 2000). Sodar can generally provide the SBL height but not always the CBL height due to inadequate height coverage. The lidars make use of aerosol extinction profiles and can provide information on diurnal variability of the ABL height. Using network of wind profilers located in California's Central Valley, Bianco et al. (2011) studied the diurnal evolution of the CBL which attains maximum height 3-4 h before the sunset. A few studies on the different ABL regimes (CBL and SBL) and their evening transition have been carried out using various remote sensing instruments located at Gadanki (Kumar and Jain, 2006; Basha and Ratnam, 2009; Kumar et al., 2012; Sandeep et al., 2015). These studies show that the mean CBL height is within 3.5 km and the mean SBL height lies below 0.6 km above the surface and their transition from the CBL to the SBL occurs about one and half hour before the sunset. However, the complete diurnal variation of the ABL height has not been reported either using single instrument or a combination of two or more.

Over Gadanki (13.45° N, 79.2° E), a tropical location in the Indian monsoon region high resolution GPS radiosonde launchings were carried out in 3-h intervals for three consecutive days in a month during the period December 2010- March 2014. Making use of this dataset, the diurnal variability of the heights of the CBL, SBL and RL (of the ABL) have been studied and the results are presented in this paper. Section 2 describes the data and methodology, results are presented in section 3, and in section 4 discussion and concluding remarks are presented.

2 Data and Method of analysis

2.1 GPS Radiosonde data

As part of Tropical Tropopause Dynamics (TTD) experiment under CAWSES-India program, intensive campaigns of high resolution GPS radiosonde were conducted to study the diurnal variability of the ABL over a tropical station, Gadanki, located at 375 m above mean sea level. The radiosondes were launched continuously at 3-h intervals for 3 consecutive days in each month from December 2010 to March 2014, except during March 2011, December 2012, January-February 2013 and April 2013. Each campaign started at 1100 IST(=UTC+0530) on day one and ended at 0800 IST on the day four. Table 1 shows the dates of radiosonde launchings. In total 764 profiles of temperature, pressure, relative humidity and horizontal wind are obtained from the 34 campaigns. These data are collected using 'Meisei RD-06G' radiosonde observations sampled at 10 m (sampled at 2 Sec intervals) under the TTD campaigns (Ratnam et al., 2014). The observed data set is gridded uniformly at to 30 m altitude resolution interval so as to remove any outliers arising from random motions or very high frequency fluctuations but the same time



to retain the ABL signature. Note that gridding these data to coarser resolution (e.g. 100 m) smooths out the ABL detection, especially the SBL, which lies generally below 0.5 km above ground level. Quality
110 checks are then applied to remove any further outliers arising due to various reasons to ensure high quality in the data (Mehta et al., 2011).

2.2 Infrared Brightness Temperature (TBB) data

Infrared Brightness Temperature (TBB) obtained from the Climate Prediction Centre, NOAA which available at a time resolution of one hour and at a spatial resolution of $0.03^\circ \times 0.03^\circ$ is used to infer the
115 cloud top height (CTH). This is globally-merged, full-resolution (~4 km) IR data formed from the ~11 micron IR channels aboard the GMS-5, GOES-8, Goes-10, Meteosat-7 and Meteosat-5 geostationary satellites. The data have been corrected for zenith angle dependence to reduce discontinuities between adjacent geostationary satellites. For this study, we averaged the TBB data into 0.25° latitude \times 0.25° longitude around Gadanki and collected for every three hours during each campaign. The cloud top height
120 is obtained as altitude corresponding to averaged TBB from radiosonde temperature profiles.

2.3 Method of analysis

Altitude profiles of temperature variables and moisture variables obtained from radiosonde observations are used to estimate the ABL height based on different methods. Seven different methods, two using the temperature profile, three using the moisture profile and two a combination of temperature and moisture
125 are adopted to estimate the ABL height in each sounding. The temperature variables are dry air temperature (T), potential temperature (θ) and moisture variables are relative humidity (RH), specific humidity (q) water vapor pressure (P_w). A combination of both temperature and moisture variables are virtual potential temperature (θ_v) and radio refractivity (N). The ABL height is generally identified as the location of (1) the maximum vertical gradient of one of the variables: T , θ , and θ_v , or (2) the minimum
130 vertical gradient one of the variables: RH, q , P_w , and N (Sokolovskiy et al., 2006; Basha and Ratnam, 2009; Seidel et al., 2010; Chan and Wood, 2013) below 3.5 km above the surface. We limited the altitude region to 3.5 km, following Chan and Wood (2013) who used GPS radio occultation refractivity data to study the seasonal cycle of the ABL over the globe. The upper limit 3.5 km is selected in order to avoid the midlevel inversions, if any. When more than one peak in the gradient occurs below 3.5 km, the lowest
135 peak having a value greater than 80% of the main peak is considered as the ABL top. As suggested by Ao et al. (2012), the gradient based ABL definitions are most meaningful when they are large in magnitude relative to the average gradient. They defined the “sharpness parameter” as $X'_s = | -X'_{min\ or\ max} / X'_{RMS} |$ where X is moisture or temperature variables and X'_{RMS} is the root-mean square (RMS) value of X' over the altitude range 0-3.5 km. If $X'_s \geq 1.25$ it is considered that ABL is
140 well defined. In the case of SBL the gradient at the top of the residual layer is much stronger than that of the gradient at the SBL. The SBL is generally identified using surface based inversion methods (Seidel et al., 2010). At the SBL, where temperature increases sharply, the temperature gradient shows a maximum value immediately just above the surface, but not at the actual level where the temperature reverses from



the positive to negative gradient. In the present study, the SBL is identified as the level of maximum
145 temperature below 0.9 km. The upper limit for the SBL height identification is based on Kumar et al.
(2012), who observed the maximum wind speed (sporadic region) deep enough up to ~0.9 km.

Following the above criteria, we have obtained the CBL, SBL and RL heights during each campaign
listed in Table 1. Out of 764 profiles, 17 profiles are rejected due to bad data quality. In the night time two
types of profiles are observed; one in which the SBL is present and other in which the SBL is not present.
150 The profiles for which the SBL is defined, are further subdivided into two cases; i) with the RL not
defined and ii) the RL defined. As the observations are at 3-h intervals, actual changes happening during
the morning transition (MT) and evening transitions (ET) during the course of diurnal cycle might not
have been captured. Sandeep et al. (2015) have made a comprehensive study on the transitory nature of
the ABL during ET over Gadanki. They found that the transition follows a top-to-bottom evolution. Note
155 that the mean sunrise time is about 0545 IST (0630 IST) while sunset time is about 1830 IST (1745 IST)
during the summer (winter) over Gadanki.

3 Results

3.1 Topography, balloon trajectory and mean wind pattern over Gadanki

Figure 1a shows the seasonal mean trajectories of balloon below 4 km and locations of balloons at 4 km
160 during different seasons launched over Gadanki for the period December 2010-March 2014. Gadanki is
surrounded by hills of maximum height of 500-600 m above the mean sea level. Towards west of the
Gadanki is the chain of the Nallamala hills with height about 800-1000 m and east side of it is flanked by
Bay of Bengal. Note that Gadanki is a far inland station (~120 km away from the Bay of Bengal coast)
and hence does not have any local effect due to the sea. The balloon generally has drifted about 0.1° and
165 0.2° in latitude and longitude, respectively. It can be seen that balloon ascends almost vertically and has
drifted towards the southwest direction during winter season (DJF; December- January-February) while
during summer monsoon season (JJA; June-July-August) they are drifted mostly towards southeast
direction. During pre-monsoon (MAM; March-April-May) balloon ascends almost vertically up to 1 km
and drifts southward above up to 4 km. In the post-monsoon months (SON; September-October-
170 November) it ascends almost vertically up to 2-3 km and change direction towards southeast.

Figures 1b-c show the seasonal mean zonal (U) and meridional (V) winds, respectively, obtained using
averaging horizontal wind data observed during the period December 2010- March 2014. Within the
ABL, it can be seen that the zonal winds are mostly easterly during the winter and pre-monsoon while
westerly during summer monsoon and post monsoon and the meridional winds remain southerly
175 throughout the year. During the summer monsoon season, low level westerly jet (LLJ) core of 10 m/s at 1
km is clearly evident.



3.2 Identification of the ABL (CBL and SBL) from temperature and moisture profiles

Figure 2 shows the typical profiles of the temperature variables T , θ , θ_v and the moisture variables RH, q , P_w and N observed at 1100 IST on 8 February 2011 to identify the CBL. Note that these profiles are
180 observed in clear sky conditions (TBB \sim 295 K). It can be seen that the CBL is capped by the inversion layer of thickness 0.150 km where a sharp increase in temperature and a sharp decrease in the moisture variables occur. The base of the entrainment zone is at 0.69 km above the ground level, which is defined as the top of the CBL. Within the CBL, θ , θ_v , and q and P_w are almost constant with altitude signifying that the air is mixed or having a tendency towards vertical mixing due to the action of the convective
185 turbulence, a characteristic of the ‘mixing layer’ (Seibert et al., 2000). Above the CBL and within the entrainment zone T , θ and θ_v increase sharply by about 1.5 K, 3.0 K and 2.0 K, respectively, and moisture variables (RH, q , P_w and N) decrease sharply by about 6 times. At the top of the entrainment zone, θ_v coincides with θ as water vapor concentration becomes very small. These sharp changes at the CBL top are easily captured by the gradient of the temperature and moisture variables as shown in Figs. 2b and 2d,
190 respectively. Both the maximum gradient of the temperature variables and the minimum gradient of the moisture variables identify the CBL height quite well.

As mentioned earlier, after sunset (in the nighttime) the identification of the SBL is not easy as the identification of the CBL, mainly because of the absence or delay in the formation of the surface inversion due to weak surface cooling. Therefore, whenever the SBL is not present the ABL is
195 represented as the RL. Typical examples of identification of the SBL are shown in Figs. 3a-3l for three different types of nighttime temperature (T , θ and θ_v) and moisture (RH, q , P_w and N) profiles and their corresponding gradient profiles indicating the presence of the SBL but not the RL, both the SBL and the RL, not the SBL but the RL, respectively. The temperature and moisture profiles and their corresponding gradient profiles observed at 0200 IST on February 9, 2011 show the evolution of the SBL only but not
200 the RL (Figs. 3a-3d). The gradients of temperature profiles and moisture profiles shown in Fig. 3b and Fig. 3d are offset by scale 10. These profiles are observed during fair weather conditions (TBB \sim 295 K). The top of the SBL identified based on the surface based the inversion (SBI) in the T is indicated as a horizontal dashed line in Fig 3a. The SBL is identified at 0.39 km above the ground level. Within the SBL both θ and θ_v increase steeply. The temperature gradient profiles show a maximum gradient at the surface which steeply decreases within the SBL (Fig. 3b). The moisture profiles (Fig. 3c) also show a steep decrease within the SBL. However, their gradients (Fig. 3d) show a negative peak at 0.18 km observed at
205 a lower height when compared to top of the SBL. The negative gradient peaks in the moisture variables are denoted as open circles. These sharp changes in the moisture variables in the SBL are indicative of inversion forming adjacent to the surface similar to the formation of entrainment zone aloft in the development of the CBL. Thus, one can also identify the height of the SBL based on moisture gradient
210 peaks (especially when temperature observation is not available) near the surface when the RL is absent. However, it becomes difficult when the gradient aloft is strong as will be seen in the later examples.

A similar feature can be noticed in the case of the SBL forming beneath the RL as identified using temperature and moisture variables, shown in Figs. 3e-3h observed at 0200 IST on December 19, 2013.



215 These profiles are observed under deep convective case with the TBB value about 262.3 K and
corresponding CTH is 6.67 km. In this case, the SBL based on the SBI is identified at 0.21 km above the
ground level (Fig. 3e). The temperature variables increase and moisture variables decrease in the SBL
(Figs 3e and 3g), but not as steep as previous profiles shown in Figs. 3a and 3c, respectively. The gradient
method identifies the RL top at 1.35 km denoted by open circles as shown in Figs. 3f and 3h. The RL has
220 similar features as the CBL mentioned in Fig 2. One can observe a weak gradient in the moisture
variables (Fig. 3h) at 0.30 km. It can be assigned as the top of the SBL defined using the gradient method
in the moisture, which is slightly higher than the SBL defined using surface based inversion. However,
identification of the negative gradient peak in the moisture profiles becomes difficult when strong RL is
present as can be noticed from the next example.

225 Unlike the above mentioned cases, an example indicating no SBL formation beneath the RL in both
temperature and moisture profiles observed at 0200 IST on February 26, 2014 is shown Figs. 3i-3l. In this
case, the feature of the RL is similar to that shown in Fig. 2 for the CBL and that shown in Figs. 3e-3h
for the RL. Like CBL, it also starts from the surface. By definition the RL is the layer observed above the
SBL and hence not considered as the ABL. However, if the SBL is absent as in this case, the RL will be
230 above the surface and it is nothing but nighttime ABL. In a study more similar in concept to ours, Liu and
Liang (2010) pointed that such cases is generally identified with near-neutral conditions in the surface
layer which they assigned as the neutral RL (NRL) that starts from the ground surface. However, in our
study, we refer to it as the RL. Using gradient method, the top of the RL is identified at 1.47 km from the
temperature variables and at 1.14 km from the moisture variables. The moisture profiles and its
235 corresponding gradients are disturbed for about 1.0 km above the RL. Unlike the previous examples, the
moisture profiles in this case do not sharply decrease. The TBB at 0200 IST on February 26, 2014 is
289.4 K and corresponding CTH of 0.81 km, indicating the presence of the low level fair weather clouds.
The RL height difference observed using temperature and moisture variables is difficult to explain, but
seems related to the effect of the cloud. The absence of the SBL indicates lack of sufficient surface
240 cooling which could be due to presence of cloud above radiatively warming the surface. It is to be noted
that there is a weak gradient present in both temperature and moisture variables at 0.51 km which is very
small when compared to the gradient at the RL. Comparing the moisture gradients below the RL top
shown in Fig. 3l with that presented in Fig. 3h, it is inferred that the gradient below the RL may not
always be due to surface cooling. Hence, identifying the SBL using moisture variables based gradient
245 method needs caution. Thus, in the present study, we preferred the identification of the SBL based on the
SBI only.

3.3 Typical diurnal variation of the ABL

From the previous typical examples presented for particular times, it is observed that the ABL identified
using temperature and moisture variables independently agree fairly well. Thus, any one temperature
250 variable and any one moisture variable are sufficient to document the ABL variation. It is also observed
that the ABL heights are well identified during different cloudy conditions. Thus, hereafter we only



examine T , θ_v , q and N for the analysis. θ and RH and P_w are dropped from further analysis as they are related to θ_v and q , respectively. The typical examples of the three hourly variations of the CBL, SBL, RL and CTH observed over three days are shown in Figs. 4a-4d for four different types of diurnal variation indicating formations of well-defined SBL, delayed SBL, no SBL, and intermittent SBL, respectively. Figs. 4a-4d also show four different cloudy conditions occurring around the ABL, far above (deep convection) the ABL, below the ABL and just above the ABL, respectively. First three (Figs. 4a-4c) panels show the complete 3 days observations for which the typical examples of the particular times have been described earlier in Fig 2 and Fig 3. Note that the diurnal variability of the CBL and RL is identified based on T , θ_v , q and N variables, while the SBL is identified using T only.

Figure 4a shows the perfect diurnal evolution of the ABL for all the 3 days observed during February 8-11, 2012 (see supplementary Fig. S1, which depicts the corresponding vertical profiles T , q and N along with TBB and CTH). It is observed that the CBL height just before noon (1100 IST) is at height 0.69 km on the first day, which further grows to height 1.2 km during afternoon (1400 IST) owing to the maximum surface heating and remains at the same height till evening (1700 IST) just before the sunset (1816 IST). During this time ET takes place and development of the SBL started at height 0.48 km at 2000 IST, which descends slowly during its nighttime evolution to the height 0.15 km at 0800 IST on the second day. Due to development of convective turbulence after the sunrise (0639 IST), the SBL is in the stage of the disappearance after 0800 IST, probably indicating the activity of MT. During the second and third days, the evolutionary feature of CBL and SBL are similar to that on the first day; however, they show large day to day variability. The CBL was not identified either by using moisture or by temperature variables at 1100 IST on second day (Fig. S1). Either clear sky conditions or the CTH below the CBL is observed during the first and third days (TBB ~ 295 K). During the second day, TBB reduced by about 10 K indicating presence of low level clouds with CTH at 2.5 km. The diurnal variation of the ABL shows the CBL at the same height using all the variables on the first day, but they differ on the second and third days. The CBL height from the minimum gradients of q and N are exactly same, indicating the dominance of the moisture part in the N when compared to T . Similarly, both T and θ_v identify same heights of the CBL and RL indicating dominance of temperature in θ_v when compared to moisture. The RL is not observed on the first night; it appears on the second and third nights, which generally decreases in the course of the night.

A similar example of typical 3 days diurnal variation of the ABL identified using T , θ_v , q and N profiles in which the SBL formation delay observed during December 18-21, 2013 is shown Fig. 4b (see corresponding vertical profiles in Fig. S2). This case is observed during deep convection events. In this case, the CBL height just before noon is at 1.59 km and remains at about the same height till evening. After the sunset, the CBL does not collapse until midnight and the SBL has not formed, indicating delay in ET process. Thus, the ABL heights observed at 2000 IST and 2300 IST are the RL top heights. The SBL appears at height 0.18 km after midnight (0200 IST) and remains at about the same height till morning (0800 IST) on the second day. On the second day, the CBL reappears again at 1.35 km before noon, which became maximum (1.83 km) afternoon and steadily decreases to 1.53 km at 2000 IST. The



290 ET process again delayed and the SBL did not form until just before the midnight on the second day. On
the third day, the CBL varies in similar fashion as on the second day but this time the ET process does not
delay and the SBL formed on 2000 IST. On the third night, the SBL at height about 0.45 km. Note that
both the temperature and moisture profiles show wave like feature during 2000 IST-0800 IST on third
night could be either due to strong horizontal advection or due to gravity wave propagation (Fig S2)
295 which will be examined in a separate study. The RL during all three days remain about the same height in
contrast to previous example where it decreases as the night progresses.

The TBB lies between the range 285 K to 218 K corresponding to the CTH about 2.46 km to 11.6 km,
respectively. By the first day (December 18, 2013) to till the evening of the third day (December 20,
2013), deep convection prevails with the CTH above 6 km except a few occasions when it lower down to
300 about 3.0-4.0 km. From midnight of the third day CTH observed below 3.0 km, during which T , q and N
were observed disturbed (Fig S2). The delay in the ET processes seems related to warming caused by
cloudy skies, which might have resulted in a delay of the surface cooling during the early part of night of
first and second day. It can be seen that, during the deep convection case, the ABL identified using
different moisture and temperature variables is the same.

305 Another typical 3 days variation of the ABL, where the SBL is not formed throughout the observation
period and when the cloud lying below the ABL as shown in Fig 4c is observed during February 24-27,
2014 (See Fig S3 for vertical profiles). Thus, during nighttime only the RL is defined which is above the
surface and considered as nighttime ABL. None of the temperature profiles show the evolution of the SBL
(Fig S3). The ABL is at about 2.0 km (1100-1700 IST) which descends down to height 1.14 km (2000
310 IST) and to 660 m (2300 IST) following ET before midnight on the first day. The CTH indicates the
presence of low level cloud at about 1.0-1.5 km since the evening of the first day to early morning of the
second day. During these cloudy days, the ABL heights (~1.5 – 2.5 km) are higher than when compared
to the ABL height (0.6-1.5 km) determined during clear sky days. An example of the typical 3 days
variation of the ABL, where SBL is defined intermittently and when cloud lying above the ABL is shown
315 in Fig 4d observed during May 29-June 01, 2012 (See Fig. S4 for vertical profiles). By intermittent is
meant the SBL defined for a few times and not the whole night. In this case, the TBB lies between the
range 290 K to 276 K corresponding to the CTH about 1.96 km to 3.60 km, respectively. The CTH is
always above the ABL. On the first day, the SBL does not form and the ABL is almost at about the same
height till the evening of the second day. On second and third nights the SBL formed for sometimes. In all
320 the above cases, the SBL either has decreased after midnight or remained constant. These two types of the
SBL are somewhat equivalent in types reported by Kumar et al., (2012). During clear-sky conditions, the
constant and decreasing SBL height after midnight are generally accompanied by steady and unsteady
winds (Kumar et al., 2012).

3.4 Correlation analysis

325 The typical examples of the SBL, CBL and RL identification shown in previous section reveal that the
different methods agree well except in a few cases. In order to see the overall correlation of the CBL and



RL heights detected from T , θ_v , q and N , a statistical comparison between them has been made as shown in Fig. 5. The total number of observations available during daytime (0800 IST -1700 IST) is 379. Out of them, the CBL is defined in 360 profiles (see Table 1), in 18 profiles the CBL is not defined and one profile is rejected due to bad data quality. The total number of observations available during nighttime (2000 IST-0500 IST) is 385. Out of them, the RL is defined in 320 profiles as listed in Table 1, in 49 profiles the RL is not defined and 16 profiles are rejected due to bad data quality during the quality check process. Figs. 5a-5d show the scatter plots of the CBL heights obtained using four different methods.

The correlation between the CBL heights obtained from T and θ_v ($r = 0.97$) (Fig. 5a) and q and N ($r = 0.99$) (Fig. 5d) are found to be excellent, which have a standard deviation (SD) of 0.16 km and 0.10 km, respectively, suggesting that it can be determined using either of the methods. However, the correlation between the CBL heights obtained from θ_v and q ($r = 0.79$) (Fig. 5b) and T and N ($r = 0.78$) (Fig. 5c) though agreeing well, have a large SD of about 0.39 km and 0.38 km, respectively. Several times, the CBL height determined from temperature variables is higher than that one obtained from the moisture variables. There could be various reasons for this disparity, however, whenever the temperature and moisture gradients are sharper or having significant gradients (Basha and Ratnam, 2009), both methods define unique height, but differences occur when they are not so sharp. Seidel et al., (2010) observed no correlation between the ABL heights obtained using T (elevated inversion) and the rest of the methods (θ_v , q , N). Surprisingly, they observed good correlation between θ and moisture variables (q , RH, N), but no correlation with T . In fact, θ mostly depends upon the T variation, so one would expect a good correlation between them as observed in our case.

Figures 5e-5h show the scatter plots of the RL heights obtained using four different methods. Similar to the CBL heights, the RL heights also show excellent correlation between T and θ_v ($r = 0.94$) (Fig. 5e) and q and N ($r = 0.96$) (Fig. 5h) with SD about 0.24 km and 0.17 km, respectively. The correlation between RL heights obtained from θ_v and q ($r = 0.86$) (Fig. 5f) and T and N ($r = 0.88$) (Fig. 5g) with SD about 0.32 km and 0.27 km, respectively, are comparatively better than the CBL heights. However, unlike the CBL heights, the RL heights estimated using different methods scatter uniformly about the linear fit, indicating that sometimes the RL heights obtained using temperature variables are higher than that of moisture variables and vice-versa. As we have observed excellent correlation between different methods, hereafter rest of the results will be presented using T variable only, because both the SBL and CBL can be easily estimated using this variable.

3.5 Statistics of the SBL, CBL, and RL heights

Before proceeding to the diurnal variation of the ABL, we first document the occurrence statistics of the SBL, CBL and RL and the general nature of their diurnal cycle as shown in Fig. 6. The occurrence of the SBL, CBL and RL and the occurrences of the SBL during different seasons are shown in Fig. 6a and 6b, respectively. SBL forms mainly during nighttime, except a few times during the early evening (1700 IST) and the late morning (0800 IST). The SBL occurrence dominates at nighttime (2300-0500 IST) with occurrence about 50%. At 2000 IST, occurrence of the SBL is only 33%, indicating that delay in surface



cooling for about 17% of the times. Over Gadanki, the occurrence of the SBL is less than the occurrence
365 over land in the midlatitude (North America and European regions) (Liu and Liang, 2010). The SBL
appeared at 0800 IST for about 25% of the time indicating the dominance of the surface cooling even
after (generally 2 hours after) the sunrise. As surface cooling starts well before (generally 2 hours before)
the sunset, sometimes (about 9%) SBL also forms at 1700 IST. In general, the SBL occurs more
frequently during the winter when compared to the summer monsoon season. Liu and Liang (2010) also
370 observed occurrences of the SBL a few times during midday. However, we have not observed such
occurrence over Gadanki. It is interesting to note that SBL at 0800 IST mostly formed during winter
month. During winter, when sunrise is at ~ 0630 IST surface cooling may remain strong till 0800 IST on
some days leading to the formation of the SBL. Whereas during summer monsoon season with sunrise at
about 0545 IST, surface cooling may not last till 0800 IST leading to very few occurrences of the SBL at
375 0800 IST. The CBL and RL occurrences dominate and are evenly distributed at 3-h intervals during
daytime (0800-1700 IST) and nighttime (2000-0500 IST), respectively. In contrast to Liu and Liang,
(2010), we observed the uniform occurrence of the CBL at 3-h intervals during daytime.

Figure 6c-6e shows the mean height of the SBL, CBL and RL along with their respective standard
deviations between 1100 IST -0800 IST. The mean SBL height varies between 0.16 ± 0.07 km at 2000
380 IST to 0.29 ± 0.21 km at 2000 IST. The overall mean SBL is below 0.3 km above the surface consistent
with the literature (Stull, 1998). After the sunrise, the CBL starts to form which lies between 1.4 ± 0.62
km at 0800 IST to $\sim 2.0 \pm 0.5$ km at 1400 to 1700 IST (Fig. 6b). Overall the mean CBL height is well
below the 3.0 km above the surface consistent with the literature (Stull, 1988; Garratt, 1994). The daytime
CBL remains prevalent as part of the RL during nighttime, which slightly falls to 1.8 ± 0.67 km at 2000
385 IST and becomes minimum 1.6 ± 0.55 km at 0200 IST (Fig. 6c).

We examine the probability distributions in order to find out the most probable height at which the
SBL, CBL and RL occur in winter, summer monsoon seasons and in the whole year as shown in Fig. 7.
Figs. 7a-7c show the SBL height distribution which has a clear peak at 0.15 km in the annual as well as
during winter and summer are lower than the mean SBL height. Both maximum distributions and mean
390 indicates that the SBL heights are within the 0.30 km as consistent with the literature except a few times
when SBL forms above it. The mean SBL height shows clear seasonal variation with lower height during
the summer than the winter season. Figs. 7d-7f show the CBL height, which has clear peaks at about 2.0
km in the annual and winter season closely coinciding with the mean CBL. During the summer season,
the CBL height distribution shows a broad peak between 0.8 km and 2.4 km, and the mean CBL height is
395 slightly higher than that during the winter season. A clear seasonal variation is also observed in the mean
CBL height. It also indicates that CBL heights are highly variable during summer monsoon season when
compared to winter season. The RL height distribution is similar to the CBL height distribution in the
annual and winter peaking at a lower height ~ 1.8 km (Figs. 7g-7h). During the summer monsoon season,
the RL height distribution shows a peak at 0.8 km in contrast to the CBL distribution. Liu and Liang
400 (2010) also observed similar distributions as observed in this study.



3.6 Diurnal and Seasonal Variation of the ABL height

We have two combinations of the ABL variability; one is the CBL and the SBL denoted as the ABL_{CS} and another is the CBL and the RL denoted as the ABL_{CR} . The diurnal variation of the ABL_{CS} height, ABL_{CR} height and the surface temperature are shown in Fig. 8. The surface temperature is taken from the automatic weather station (AWS) observations over Gadanki. The diurnal variation of the ABL comprises of the CBL observed between 0800 IST and 1700 IST, the SBL at 1700 IST and 0800 IST and the RL observed between 2000 IST and 0500 IST. As mentioned earlier, the mean CBL varies between ~0.5 km and 3.0 km and the mean SBL varies between ~ 0.09 km and 0.6 km. The mean diurnal variation of the CBL and the SBL (ABL_{CS} hereafter) shows that the CBL evolved slowly with time attains maximum height at 1400 IST and either remains constant or decrease slowly till 1700 IST and then collapse to the SBL. The mean variation of the SBL over time is very small. It can be seen that the ET is more abrupt at 1700 IST than the morning rise at 0800 IST consistent to earlier studies (e.g. Liu and Liang, 2010).

The variation of the CBL and RL (ABL_{CR} hereafter) over three days for all the campaigns is shown in Fig. 8b. Note that the CBL variation at 1700 and 0800 IST presented in Fig 8a is relatively lower because former also includes the SBL observations; especially during 1700 IST and 0800 IST (see Fig 6). It is interesting to note that the RL falls to lower height most of the night and thus, the ABL_{CR} shows a diurnal pattern with maximum height during 1700 IST and minimum during early morning 0800 IST. The observed maximum height of the CBL at 1700 IST is found to be consistent with the general circulation model output (Medeiros et al., 2005). The RL height varies from ~0.5 km to ~3.0 km. The RL is present throughout the night during most of the day, which is sustained by the presence of the relatively warm air trapped between two stable layers, RL at the top and recently developed SBL due to surface cooling at the bottom. The trapped warm air slowly becomes cooler due to exchange of heat to the adjoining free atmosphere and gradually intensifying SBL results in the descent of the RL during the course of the night, allowing the turbulence to decrease homogeneously in all directions. Diurnal variation of the ABL_{CR} shows a similar pattern as the surface temperature. The surface temperature attains maxima at 1400 IST and minima at 0200 IST.

Figure 9 shows the diurnal variation of the ABL height (obtained using T variable) and surface temperature during different seasons. We have considered those cases which show the diurnal pattern of the ABL i.e. the formation of the CBL during daytime and SBL during nighttime as well as all those cases whenever SBL forms intermittently (excluding RL). As mentioned earlier, note that the occurrence frequency of the SBL just after the sunset is less than that of later periods at night. It means that the SBL has not formed always immediately after the sunset. Several times, formation of the SBL delay by 3-4 hours after the sunset. Thus, we cannot expect a perfect diurnal variation in all the cases, especially when the SBL formation is delayed. In order to study the diurnal variation of the ABL, we have segregated all the CBL and SBL observed at 3-h intervals during the diurnal cycle in different seasons. Similarly, all the cases of the CBL and RL observed at 3-h intervals are averaged into different seasons.

Figures 9a-9b show the diurnal variation of the ABL_{CS} and ABL_{CR} during different seasons. In general, the CBL heights vary between 1.05 ± 0.46 km to 2.25 ± 0.72 km, the SBL heights vary between 0.15 ± 0.05



km to 0.33 ± 0.27 km and the RL heights vary from 1.39 ± 0.41 km to 1.94 ± 0.63 km. We have also obtained
440 the diurnal variation of the surface temperature during different seasons as shown in Fig 9c. In general,
the diurnal patterns of the ABL_{CS} and ABL_{CR} during different seasons are same as annual mean pattern
shown in Fig 8a and Fig 8b, respectively. The diurnal variation of the ABL_{CS} shows a seasonal pattern
such that CBL attain maximum height during the summer monsoon while the SBL during the winter to
pre-monsoon. The amplitude of the diurnal evolution of the ABL_{CS} is stronger during pre-monsoon when
445 compared to other seasons, i.e. maximum to minimum height variation is more during pre-monsoon when
compared to other seasons. The SBL attains maximum height at 0200 IST. Fig 9b shows that the ABL_{CR}
height has a weak diurnal pattern during the winter when compared to summer. It is interesting to note
that the CBL and RL heights reverse their seasonal pattern. The CBL height is higher during summer and
is lower during winter in contrast, to the RL height, which becomes higher during winter and lower
450 during summer. In general, the CBL attains maximum height at 1400-1700 IST and minimum during
0800-1100 IST during all seasons.

Figure 9c shows the diurnal variation of the surface temperature during different seasons; surface
temperature is highest and lowest during pre-monsoon and winter, respectively. The highest amplitude of
the diurnal variation of the ABL_{CR} can be attributed to highest surface temperature during pre-monsoon.
455 Similarly, the weak diurnal pattern of the ABL_{CR} can be attributed to the lowest surface temperature
during the winter.

3.7 Qualitative relationships between cloud top height (CTH) and ABL_{CR} height

The presence of the clouds has a large impact on the boundary layer structure. However, it leads to
460 considerable complication because of the important role played by radiative fluxes and phase change
(Garratt, 1992). The relationship between the CTH and the CBL/RL is obtained and is shown in Fig. 10.
We have observed the CTH at various layers ranging from within the ABL to up to 12 km during the
different campaigns. The CTH relative to the ABL_{CR} is obtained for each individual campaign, which is
listed in Table 1. In total, for 630 cases the clouds were present either below or near to or above the
465 ABL_{CR} . Rest of 50 cases are when the clear sky conditions observed. Note that in total 680 cases, when
CBL and RL are defined. We observed that in total 175, 199, 222 and 34 cases, when CTH occurred
within ± 0.5 km, below 0.5 km, above 0.5 km but below 6.0 km, and above 6.0 km of the ABL_{CR} ,
respectively. These cutoff heights regions are selected through visual inspection by trial and error after
examining several ABL height and CTH timeseries. The timeseries of the CTH and ABL_{CR} for the cases
470 when the CTH occurred within ± 0.5 km, below 0.5 km, above 0.5 km but below 6.0 km of ABL_{CR} are
shown in Fig 10. The CTH within ± 0.5 km of the ABL_{CR} is positively correlated ($r = 0.88$) with SD of
0.28 km (Fig 10a). Fig 10a further reveals a clear association between the ABL_{CR} and the CTH variations.
These cases indicate the cloud topped boundary layer (CTBL) where clouds are limited in their vertical
extent by main capping or subsidence inversion (Garratt, 1992). Fig. 10b shows that the CTH occurring
475 below 0.5 km of the ABL_{CR} is also positively correlated ($r = 0.71$) with SD 0.37 km. Although these



clouds occur well below the ABL_{CR} , both vary in the similar fashion (Fig 10b). It can be seen that higher the cloud level higher the ABL_{CR} and vice versa. Similarly, the ABL_{CR} height variation is also well correlated with the CTH variation occurring above 0.5 km but below 6.0 km of the ABL (Fig 10c).

It is interesting to note that when the CTH is below the ABL_{CR} , CBL and RL occur at higher height
480 (mostly above 2 km) whereas when the CTH is above the ABL_{CR} , CBL and RL occur at a lower height
(mostly below 2.0 km). Generally, the CBL (sometimes also called as fair weather boundary layer)
occurs at lower height during a shallow cumulus when compared to clear sky conditions (Medeiros et al.,
2005). Very deep convective clouds do not show any relationship with the ABL_{CR} variation (figure not
shown) as can be seen from Fig. 4b. Qualitatively, it indicates that the presence of the clouds near to the
485 CBL and RL directly impact its variation, but not the high level clouds due to the deep convection events.

4 Discussion and Conclusions

The unique and long term intensive campaigns of high vertical resolution radiosonde observations on
multiple of 3 hours over a tropical location, Gadanki, in the Indian monsoon region reveal the clear
diurnal structure of the ABL height. The high vertical resolution of the radiosonde data enables us to
490 detect the SBL height directly, which otherwise was very difficult.

Identification of the ABL is generally preferred using θ_v and q obtained from radiosonde observation
because they can represent the mixing height better than the T . However, we observed an excellent
correlation between T and θ_v , suggesting that ABL can be identified using T . Moreover, use of T can give
both elevated inversion as well as surface based inversion well suited to study the diurnal variation of the
495 ABL. The limitation of using T is that it can also identify mid-level inversion sometimes. However, to
avoid mid-level inversions, if any, we have restricted ABL height identification below 3.5 km. In case of
multiple inversions, the lower one having 80% of main inversion is considered. The correlation between
 T (or θ_v) and N are in good agreement with Basha and Ratnam, (2009). We also found that N yields the
ABL height lower than that of T several times, but not always, in contrast to Chennai located 120 km
500 southeast of Gadanki where significant ABL height difference of ~ 0.84 (between θ and N) is observed in
evening soundings (Seidel et al., 2010).

The nighttime ABL is complex to define when compared to daytime ABL. As the nighttime ABL or
the SBL depends on the surface cooling, if it delays, or does not form at all, which generally happens, one
will find the nighttime ABL as about same as pervious daytime ABL (i.e CBL). It is the part of the
505 daytime mean state and has not formed due to action of nighttime surface forcing. However, as it is above
the surface, which is an only criterion left to assign the RL as the ABL in the absence of the SBL (Liu and
Liang, 2010). But, if the measuring instrument has limited capability to detect the SBL, one will land in
defining the RL as nighttime ABL, which will not be a true representation of the ABL height.

In total, the SBL forms about 50% times during the midnight to morning. In the early part of the night,
510 the SBL occurs less frequently (33%) than late night and hence indicates the delay in the surface cooling
process. The SBL forms more frequently during winter season when compared to other seasons. Thus,



diurnal variation of the ABL occurs more often during winter than the summer. There could be various reasons for the delay in the SBL formation, such as cloud cover or wet surface due to rain which can disturb or delay the surface cooling process. Sandeep et al, (2015) observed that ABL over Gadanki after
515 sunset becomes shallower and its growth delayed by 1–4 h during wet episodes. Over Indian region, clouds and precipitation most frequently occur during the summer monsoon season when compared to the winter season, suggesting the formation of the SBL will be less frequent during the former season consistent to the observed result. However, irrespective of the season the surface temperature shows a diurnal pattern. Thus, another possibility of less occurrence of the SBL during summer monsoon season
520 could be due to high night time temperature. In fact the nighttime surface temperature during summer monsoon as well as post and pre monsoons are greater than that of daytime surface temperature during the winter season. Though, the surface temperature during these seasons decreases during nighttime, it doesn't have sufficient cooling effect as winter season probably preventing the formation of the SBL during summer. Thus, it could be possible that even though the surface temperatures show diurnal
525 variation during the summer monsoon, diurnal variability in the ABL may not be expected.

The minimum height of the CBL at 0800 IST is due to weak convection (thermals) during the morning hours when compared to other timings of the day. As convection becomes stronger (the strongest surface warming at 1400 IST) due to the strong thermals, the CBL becomes higher and reaches a maximum height at 1400-1700 IST. Similarly, as the night passes, surface cooling becomes stronger (the
530 strongest cooling occurs at 0200 IST) leading to higher SBL height at 0200 IST -0500 IST. The RL remains sometimes at similar height as the CBL in case of very strong gradient in moisture and temperature. But generally it lowers down as time passes during the night. As daytime convection is switched off during the night, the turbulence strength goes weaker and weaker as night passes leading to decrease in the RL height.

535 During the pre-monsoon, the surface temperature has the strongest diurnal variation which manifests stronger diurnal variation of the ABL_{CR} height (Angevine et al., 2001). But higher CBL occurs during the summer monsoon season and not during the pre-monsoon. The higher CBL during summer monsoon season is due to stronger convection occurring this season when compared to the other seasons. During the winter season, the surface temperature is low leading to a weak diurnal pattern of the ABL_{CR}
540 (Angevine et al., 2001). Since convection is weaker during the winter season, the CBL is at a lower height when compared to the other seasons. The reversal of the CBL and RL height patterns between summer monsoon and winter is due to the surface temperature variation and strength of convection. It is due to the fact that during the winter the RL does not lower as observed for the other seasons due to less surface temperatures, while the CBL becomes higher during summer monsoon seasons due to stronger
545 convection when compare to the winter. Thus, the CBL is lower during the winter, but it is higher during summer monsoon while RL is higher during winter but it is lower during summer monsoon season.

Finally, the qualitative relationship between the ABL_{CR} height and the CTH is examined. We only provide here qualitative information based on the CTH obtained using merged TBB data, since direct



550 observation of the CTH over the launch site during the campaign periods are not available. As observed
in this study, the CTH at various layers has been observed using ceilometer at Ahmedabad (23.03° N,
72.54° E), India (Sharma et al., 2016). If the clouds occur above the ABL_{CR} during the daytime, they will
absorb the incoming solar radiation and hence cool the surface. This in turn will weaken the thermals and
hence decrease the CBL height. On the other hand, when the clouds occur below the CBL, it will cool the
555 surface, but warm the region between cloud top and CBL and hence can strengthen the thermals which
will lead to increase the CBL height. This explains why CBL is at lower height when the clouds above it
and at the higher height when clouds below it. If cloud occurs during nighttime, the situation will be
more complex and difficult to explain the RL variability. During nighttime, the clouds will block the
outgoing long wave radiation, which in general warm below the RL and hence disturb the surface cooling
560 and the formation of the SBL. The verification of the CTH height using space borne satellites and ground
based observations such as ceilometer over the launch site will be carried out as a separate study in the
future.

Following are the main findings on the diurnal variability of the atmospheric boundary layer (ABL):

- 565 1. The convective boundary layer (CBL) height has a large variation ranging from as low as 0.4 km
to as high as about 3.0 km above the surface and occurs uniformly at 3-h intervals during the
diurnal cycle over Gadanki, a tropical station in the Indian monsoon region.
- 570 2. The stable boundary layer (SBL) mainly forms during nighttime; however, it can also form
during daytime, especially during evening and morning hours, i.e. during transition periods. The
SBL forms about 50% of times of total observations during 2300-0500 IST. At 2000 IST,
occurrence of the SBL is only 33%, indicating that delay in surface cooling for about 17% of the
times. About 25 % of the time the SBL forms at 0800 IST indicating the dominance of the
surface cooling even after the sunrise. As surface cooling starts well before the sunset,
sometimes the SBL (about 9%) also forms at 1700 IST.
- 575 3. The overall the mean SBL lies well within the 0.3 km and the mean CBL lies well with 3.0 km
consistent with the available literature. However, the maximum probability distribution of the
SBL occurs at 0.15 km lower than its mean value. In contrast to the SBL, the maximum
probability distribution of the CBL coincides with mean CBL at about 2 km for the winter
season and the whole year. The maximum probability distribution of the CBL during the summer
580 monsoon season has a broader peak when compare to winter season.
4. The CBL and the RL heights obtained using different methods (T , θ , q and N) correlates well.
5. A clear diurnal variation of the ABL_{CS} height over the different seasons is observed with the
maximum CBL height during summer monsoon season while the maximum SBL height during
winter to pre-monsoon. The seasonal pattern reverses for the RL height that becomes higher
585 during winter and lower during summer monsoon season.
6. The ABL_{CR} height is positively correlated with the CTH occurring near to it, however, the deep
convective clouds do not show any relationship. When the cloud is at lower height the ABL_{CR} is



relatively higher and vice versa. This needs to be verified using independent observations of the CTH perhaps using Ceilometer observations.

590

Acknowledgements. We thank NARL radiosonde operation team for conducting the experiment under tropical tropopause dynamics (TTD) campaigns fully supported by the Indian Space Research Organization as a part of CAWSES India Phase-II program.

References

- 595 Angevine, W. M., Baltink, H. K., and Bosveld, F. C.: Observations of the morning transition of the convective boundary layer, *Bound.-Lay. Meteorol.*, 101, 209-227, 2001.
- Ao, C. O., Waliser, D. E., Chan, S. K., Li, J. L., Tian, B., Xie, F., and Mannucci, A. J.: Planetary boundary layer heights from GPS radio occultation refractivity and humidity profiles, *J Geophys Res.-Atmos.*, 117, 2012.
- 600 Basha, G. and Ratnam, M. V.: Identification of atmospheric boundary layer height over a tropical station using high-resolution radiosonde refractivity profiles: Comparison with GPS radio occultation measurements, *J Geophys Res.-Atmos.*, 114, 2009.
- Bianco, L., Djalalova, I., King, C., and Wilczak, J.: Diurnal evolution and annual variability of boundary-layer height and its correlation to other meteorological variables in California's Central Valley, *Bound.-Lay. Meteorol.*, 140, 491-511, 2011.
- 605 Chan, K. M. and Wood, R.: The seasonal cycle of planetary boundary layer depth determined using COSMIC radio occultation data, *J Geophys Res.-Atmos.*, 118, 2013.
- Chandrasekhar Sarma, T., Narayana Rao, D., Furumoto, J., and Tsuda, T.: Development of radio acoustic sounding system (RASS) with Gadanki MST radar—first results, 2008, 2531-2542.
- Clifford, S. F., CHANDRAN KAIMAL, J., Lataitis, R. J., and Strauch, R. G.: Ground-based remote profiling in atmospheric studies: An overview, *Proc. IEEE*, 82, 313-355, 1994.
- 610 Dearnorff, J. W.: Parameterization of the planetary boundary layer for use in general circulation models 1, *Mon. Weather Rev.*, 100, 93-106, 1972.
- Garratt, J.: *The atmospheric boundary layer*, Cambridge atmospheric and space science series, Cambridge University Press, Cambridge, 416, 444, 1992.
- 615 Garratt, J. R.: Review: the atmospheric boundary layer, *Earth-Sci. Rev.*, 37, 89-134, 1994.
- Holtzlag, A. and Nieuwstadt, F.: Scaling the atmospheric boundary layer, *Bound.-Lay. Meteorol.*, 36, 201-209, 1986.
- Konor, C. S., Boezio, G. C., Mechoso, C. R., and Arakawa, A.: Parameterization of PBL processes in an atmospheric general circulation model: description and preliminary assessment, *Mon. Weather Rev.*, 137, 1061-1082, 2009.
- Kumar, K. K. and Jain, A.: L band wind profiler observations of convective boundary layer over Gadanki, India (13.5 N, 79.2 E), *Radio Sci.*, 41, 2006.
- 620 Kumar, M. S., Anandan, V., Rao, T. N., and Reddy, P. N.: A climatological study of the nocturnal boundary layer over a complex-terrain station, *J. Appl. Meteorol. Clim.*, 51, 813-825, 2012.
- Liu, S. and Liang, X.-Z.: Observed diurnal cycle climatology of planetary boundary layer height, *J. Climate*, 23, 5790-5809, 2010.
- 625 Medeiros, B., Hall, A., and Stevens, B.: What controls the mean depth of the PBL?, *J. Climate*, 18, 3157-3172, 2005.
- Mehta, S. K., Ratnam, M. V., and Krishna Murthy, B.: Multiple tropopause in the tropics: A cold point approach, *J Geophys Res.-Atmos.*, 116, 2011.
- Ratnam, M. V., Sunilkumar, S., Parameswaran, K., Murthy, B. K., Ramkumar, G., Rajeev, K., Basha, G., Babu, S. R., Muhsin, M., and Mishra, M. K.: Tropical tropopause dynamics (TTD) campaigns over Indian region: An overview, *J. Atmos. Sol-Terr. Phys.*, 121, 229-239, 2014.
- 630 Sandeep, A., Rao, T. N., and Rao, S.: A comprehensive investigation on afternoon transition of the atmospheric boundary layer over a tropical rural site, *Atmos. Chem. Phys.*, 15, 7605-7617, 2015.
- Seibert, P., Beyrich, F., Gryning, S.-E., Joffre, S., Rasmussen, A., and Tercier, P.: Review and intercomparison of operational methods for the determination of the mixing height, *Atmos. Environ.*, 34, 1001-1027, 2000.
- 635 Seidel, D. J., Ao, C. O., and Li, K.: Estimating climatological planetary boundary layer heights from radiosonde observations: Comparison of methods and uncertainty analysis, *J Geophys Res.-Atmos.*, 115, 2010.
- Sharma, S., Vaishnav, R., Shukla, M. V., Kumar, P., Kumar, P., Thapliyal, P. K., Lal, S., and Acharya, Y. B.: Evaluation of cloud base height measurements from Ceilometer CL31 and MODIS satellite over Ahmedabad, India, *Atmos. Meas. Tech.*, 9, 711-719, 2016.
- 640 Shravan Kumar, M. and Anandan, V.: Comparison of the NCEP/NCAR Reanalysis II winds with those observed over a complex terrain in lower atmospheric boundary layer, *Geophys. Res. Lett.*, 36, 2009.
- Sokolovskiy, S., Kuo, Y. H., Rocken, C., Schreiner, W., Hunt, D., and Anthes, R.: Monitoring the atmospheric boundary layer by GPS radio occultation signals recorded in the open-loop mode, *Geophys. Res. Lett.*, 33, 2006.



- 645 Stull, R. B.: An introduction to boundary layer meteorology, Atmospheric Sciences Library, Dordrecht: Kluwer,
1988, 1, 1988.
- Tucker, S. C., Senff, C. J., Weickmann, A. M., Brewer, W. A., Banta, R. M., Sandberg, S. P., Law, D. C., and
Hardesty, R. M.: Doppler lidar estimation of mixing height using turbulence, shear, and aerosol profiles, *J. Atmos.
Ocean. Tech.*, 26, 673-688, 2009.
- 650 van der Kamp, D. and McKendry, I.: Diurnal and seasonal trends in convective mixed-layer heights estimated from
two years of continuous ceilometer observations in Vancouver, BC, *Bound.-Lay. Meteorol.*, 137, 459-475, 2010.

655

660

665

670

675

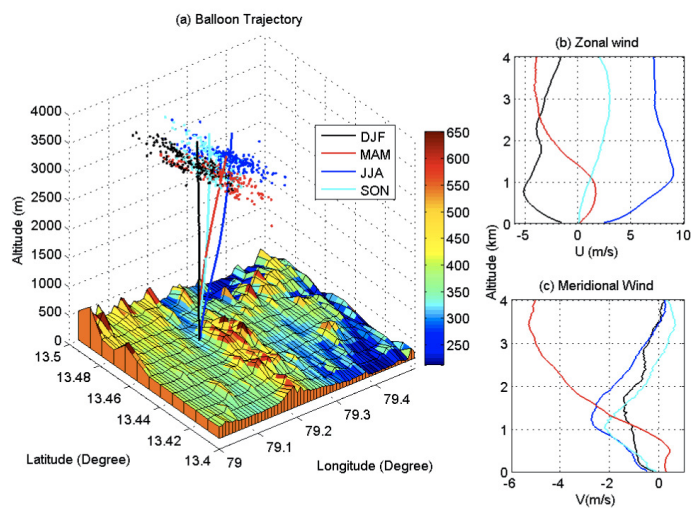
680



685 **Table 1: List of 3-days campaigns conducted during the period December 2010-March 2014. Total number of observations, rejection of bad quality data, the SBL, the CBL and the RL are listed for each campaign. Shaded regions indicate campaigns with more than 90% of the SBL defined. Bold indicates those campaigns where SBL is not defined and the rest when the SBL occur intermittently. CTH relative to ABL are also listed.**

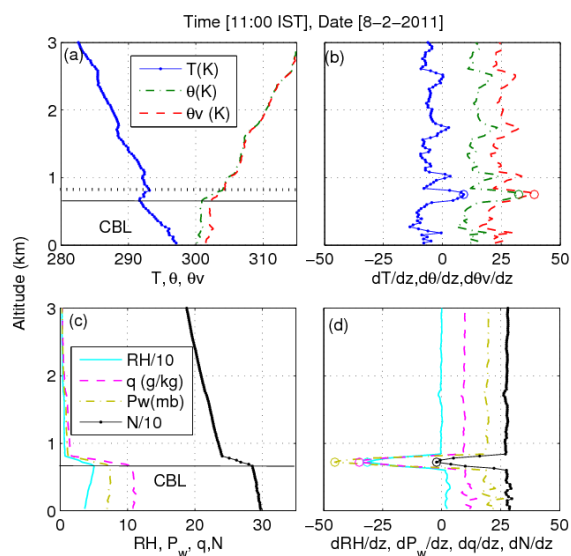
SN	Period	No of Observations					CTH-ABL
		Total	Rejected	SBL	CBL	RL	
1	28 Dec 2010-31 Dec 2010	24	0	10	12	12	±1.5
2	17 Jan 2011-20 Jan 2011	24	0	14	10	6	-2.0-1.0
3	08 Feb 2011-11 Feb 2011	24	0	14	11	7	-2.0-1.0
4	26 Apr 2011-29 Apr 2011	24	2	0	11	10	-1.0-2.0
5	18 May 2011-21 May 2011	24	1	5	8	9	-1.0-7.0
6	20 Jun 2011-23 Jun 2011	24	0	0	12	12	-1.5-1.0
7	21 Jul 2011-24 Jul 2011	24	0	0	12	12	-1.5-2.0
8	17 Aug 2011-20 Aug 2011	24	1	5	10	9	-1.5-1.0
9	12 Sep 2011-15 Sep 2011	24	1	11	12	8	±2.0
10	12 Oct 2011-15 Oct 2011	12	2	6	5	3	±0.5
11	14 Nov 2011-17 Nov 2011	24	0	13	12	12	-2.0-0.0
12	08 Dec 2011-11 Dec 2011	23	1	7	11	11	-2.0-8.0
13	18 Jan 2012-21 Jan 2012	17	1	8	7	9	±2.0
14	23 Feb 2012-26 Feb 2012	22	0	13	10	11	-1.5-2.0
15	29 Mar 2012-01 Apr 2012	23	0	0	12	11	-1.0-4.0
16	01 Apr 2012-04 Apr 2012	24	0	9	11	7	0.5-2.5
17	29 May 2012-01 Jun 2012	23	0	6	12	11	-0.5-1.5
18	26 Jun 2012-29 Jun 2012	23	0	8	10	8	-1.0-2.5
19	24 Jul 2012-27 Jul 2012	24	2	4	11	11	-1.5-1.0
20	21 Aug 2012-24 Aug 2012	23	0	8	10	6	-1.5-2.5
21	12 Sep 2012-15 Sep 2012	23	0	7	11	8	-0.5-2.0
22	03 Oct 2012-06 Oct 2012	21	0	6	11	10	±0.5
23	05 Nov 2012-08 Nov 2012	12	1	2	6	5	±0.5
24	21 May 2013-24 May 2013	22	1	6	10	10	-1.0-2.5
25	17 Jun 2013-20 Jun 2013	24	0	2	12	12	-1.0-3.5
26	15 Jul 2013-18 Jul 2013	24	0	5	12	12	-1.0-2.0
27	26 Aug 2013-29 Aug 2013	24	0	5	11	7	-1.5-0.5
28	23 Sep 2013-26 Sep 2013	24	0	4	11	6	±1.5
29	28 Oct 2013-31 Oct 2013	21	0	6	11	9	-2.0-5.0
30	21 Nov 2013-24 Nov 2013	19	2	0	8	9	-2.0-5.0
31	18 Dec 2013-21 Dec 2013	24	0	11	12	12	1.0-11.0
32	27 Jan 2014-30 Jan 2014	24	0	0	12	12	-0.5-(-2.0)
33	24 Feb 2014-27 Feb 2014	24	0	0	12	12	-2.0-0.5
34	25 Mar 2014-28 Mar 2014	24	1	12	12	11	-1.0-7.0
	Total	764	17	207	360	320	

690



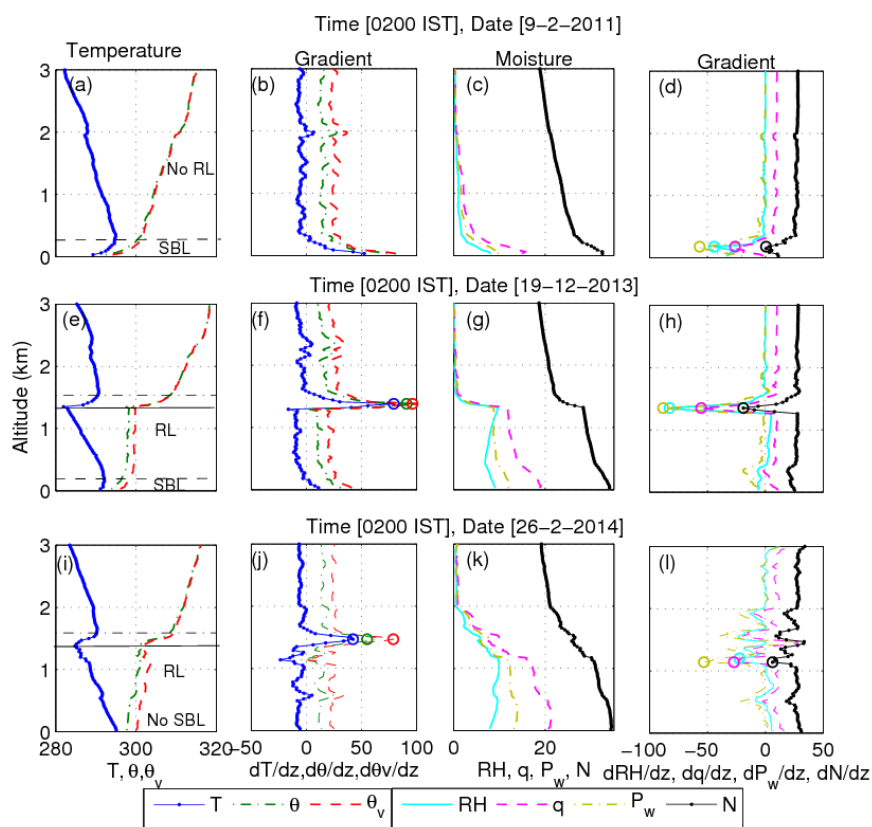
695 Figure 1: (a) Topographical features surrounding the location of radiosonde launch site, Gadanki (13.45° N,
79.2° E), a tropical station, India, along with profiles of seasonal mean trajectories (thick lines) from the
surface to 4 km and the locations of the balloon reaching at altitude 4 km (dots) during different seasons. The
mean (b) zonal wind and (c) meridional winds for different seasons observed during the period December
2010-March 2014. Global 30-arc-second gridded topography data is provided by the National Centers for
700 Environmental Information, USA.

705

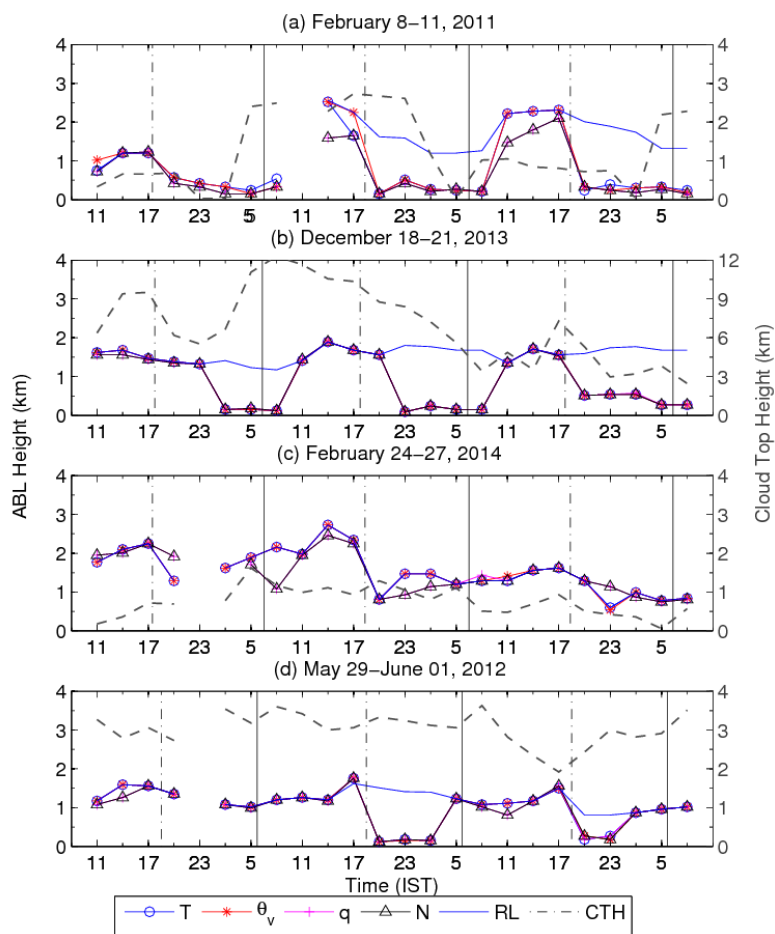


710 **Figure 2:** Typical profiles of (a) temperature (T), potential temperature (θ) and virtual potential temperature (θ_v) and (c) relative humidity (RH), specific humidity (q), water vapor pressure (P_w), and radio refractivity (N) showing convective boundary layer (CBL) using GPS radiosonde observation at 1100 IST on February 8, 2011 over Gadanki (13.45° N, 79.2° E). (b) and (d) show the gradient profiles corresponding to (a) and (c), respectively. Solid horizontal lines in (a) and (c) indicate the base of the inversion layer, respectively. Dotted line in (a) indicates the top of the inversion. Open circles in figures (b) and (d) denote the CBL heights above ground level.

715



720 Figure 3: Same as Figure (2) but for night time profiles observed at 0200 IST indicating (a) the stable boundary layer (SBL) only, but not the residual layer (RL) observed on February 9, 2011, (b) both the SBL and the RL observed on December 19, 2013 and (c) the RL but not the SBL observed on on February 26, 2014. The horizontal dashed lines denote the surface based inversion in the temperature profile and open circles denote maximum gradients in temperature variables or minimum gradients in the moisture variables. Horizontal dash-dotted lines indicate capping inversion layer.



725 **Figure 4: Diurnal variability of the ABL (CBL, SBL and RL) height obtained from the variables T , θ , q , and N during (a) February 8-11, 2011, (b) December 18-21, 2013, (c) February 18-21, 2013, and (d) May 29- June 01, 2012. Thick dashed lines indicate the cloud top height (CTH). Vertical dashed and solid bars indicate sunrise and sunset times, respectively.**

730

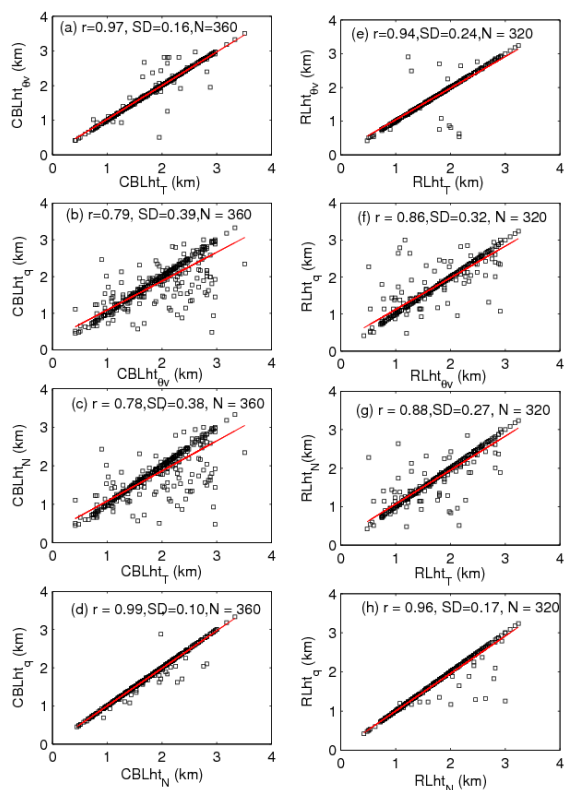
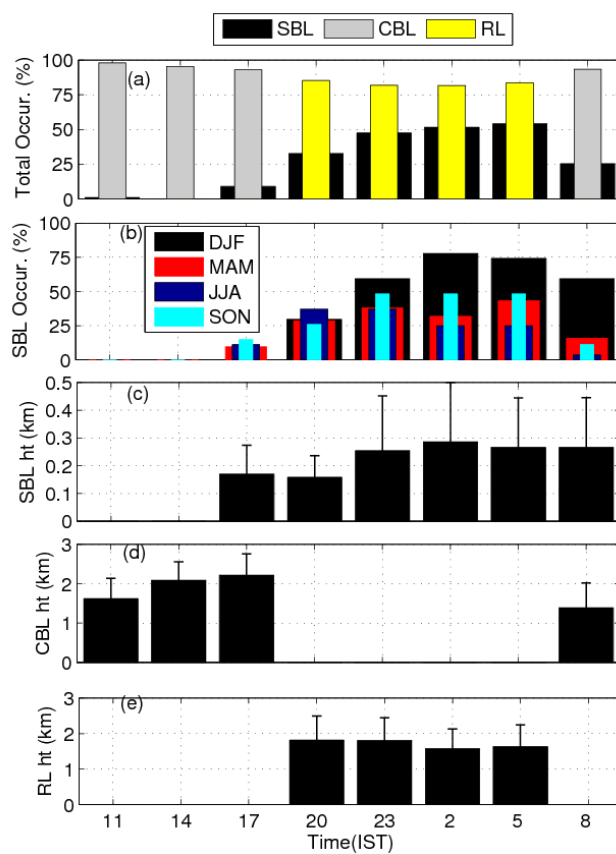
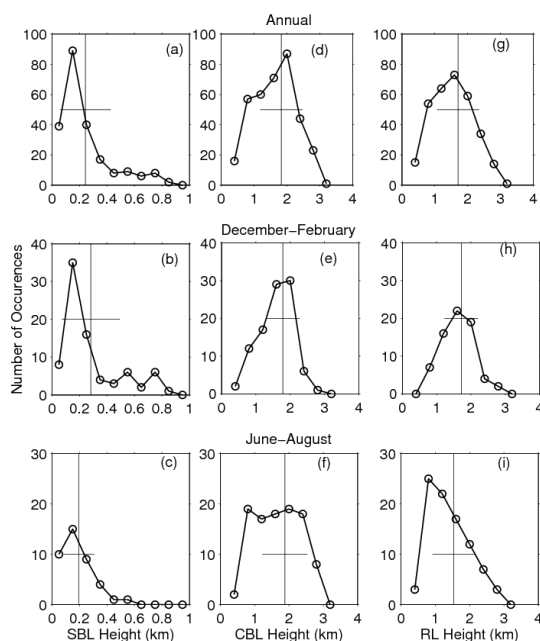


Figure 5: (Left panels) Correlation between the CBL heights obtained using (a) T and θ_v , (b) θ_v and q , (c) T and N , and (d) N and q . (Right Panels) (e)-(h) are same as (a)-(d) but the RL heights.

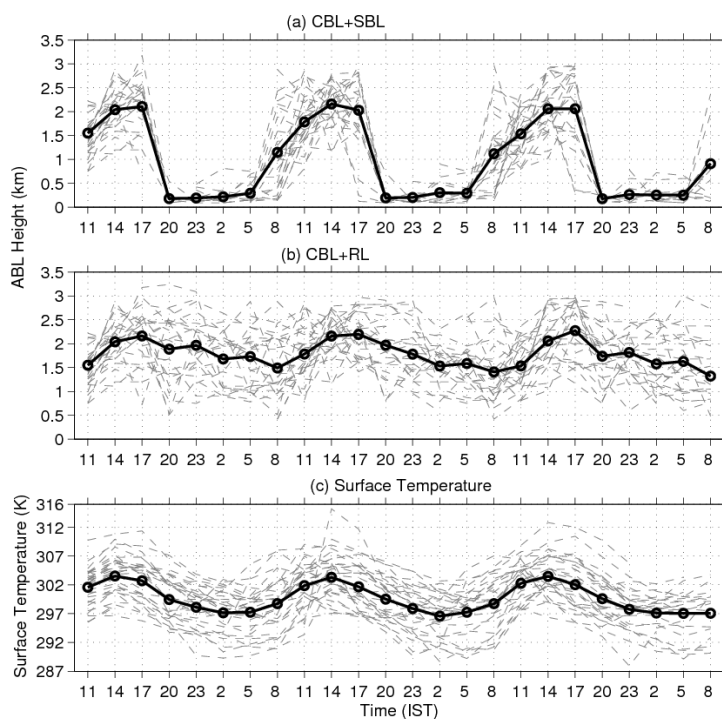


735

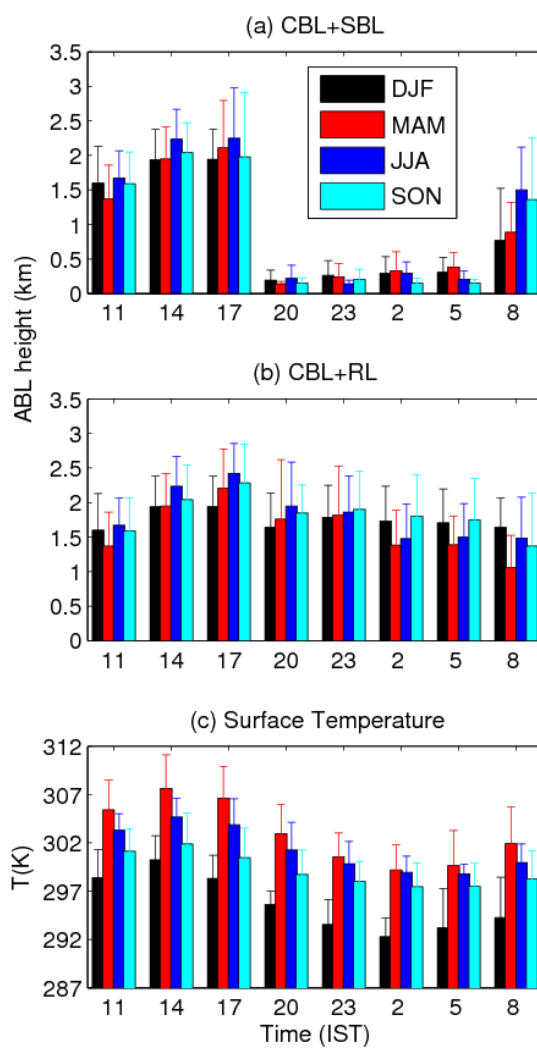
740 **Figure 6:** (a) Total percentage occurrence of the SBL, CBL, and RL heights (b) percentage occurrence of the SBL during different seasons. Mean and standard deviations of (c) the SBL height observed at 3 hours interval between 1700 IST and 0800 IST, (d) the CBL observed at 3 hours interval between 0800 IST and 1700 IST and (e) the RL observed at 3 hours interval between 2000 IST and 2300 IST. These statistics are obtained using T variables.



745 **Figure 7: Probability distribution of 3 hourly (left column panels) SBL height with 0.1 km interval obtained for (a) annual (b) winter and (c) summer from the data observed during December 2010–March 2014. (d)–(e) same as (a)–(c) but for the CBL height, and (f)–(h) are same as (a)–(c) but for the RL height with 0.4 km interval. The Points at which the vertical line intersects the x-axis represents their mean heights while the length of the horizontal bar represents the corresponding standard deviations.**

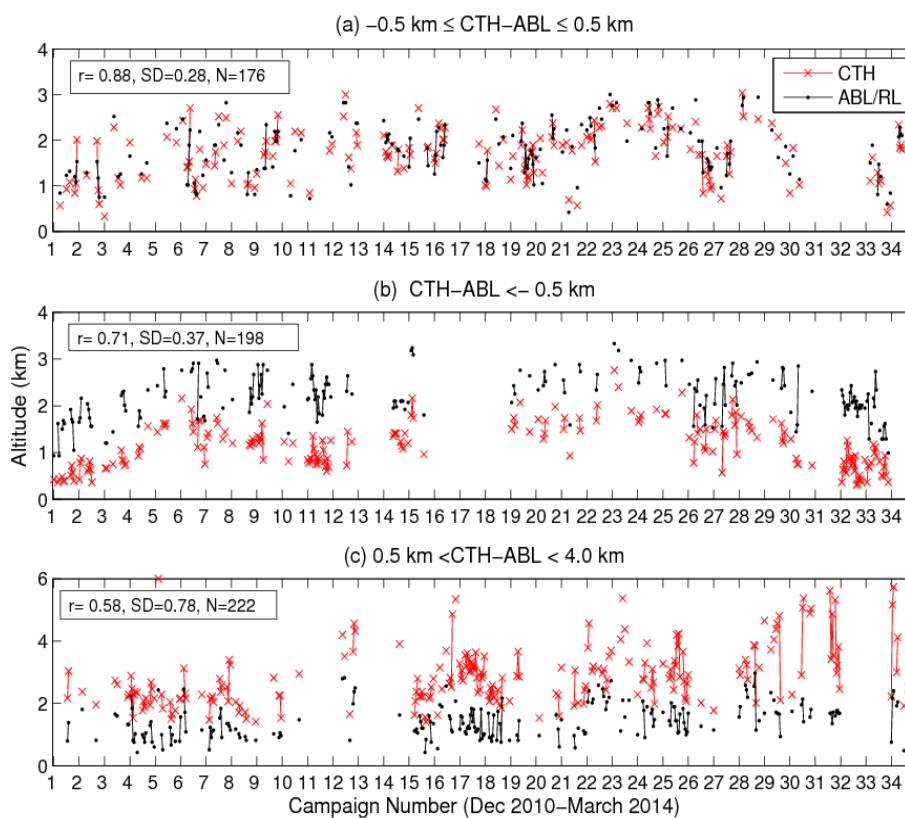


750 **Figure 8:** (a) The 3 days diurnal variability of the (a) the ABL (CBL+SBL) considering all the data observed for the CBL and SBL, (b) the CBL+RL considering all the data observed for the CBL and RL obtained using T variable, and (c) Surface temperature observed during the period December 2010-March 2014.



755

Figure 9: The diurnal variation of (a) the ABL_{CS} (CBL+SBL) height, (b) the ABL_{CR} (CBL+RL) height and (c) the surface temperature during different seasons.



760 **Figure 10:** Time series of the CTH and the ABL_{CR} top observed for the cases (a) $-0.5 \text{ km} \leq \text{CTH} - \text{ABL} \leq 0.5 \text{ km}$
(b) $\text{CTH} - \text{ABL} < -0.5 \text{ km}$ and (c) $0.5 \text{ km} < \text{CTH} - \text{ABL} < 4.0 \text{ km}$.

765